Sol−Gel-Derived BPO_4/Ba^{2+} as a New Efficient and Environmentally-Friendly Bluish-White Luminescent Material

C. K. Lin,[†] Y. Luo,[†] H. You,[‡] Z. Quan,[†] J. Zhang,[†] J. Fang,[§] and J. Lin*,[†]

Key Laboratory of Rare Earth Chemistry and Physics, State Key Laboratory of Polymer Physics and Chemistry, Changchun Institute of Applied Chemistry, Chinese Academy of Sciences, Changchun 130022, and Graduate School of the Chinese Academy of Sciences, Beijing 100049, P. R. China, and Department of Chemistry and Advanced Materials Research Institute, University of New Orleans, New Orleans, Louisiana 70148

Received September 19, 2005. Revised Manuscript Received October 25, 2005

In this paper, BPO_4 and Ba^{2+}-doped BPO_4 powder samples were prepared by the sol−gel process using glycerol and poly(ethylene glycol) as additives. The structure and optical properties of the resulting samples were characterized by X-ray diffraction (XRD), Fourier transform infrared (FT-IR) spectroscopy, field emission scanning electron microscopy (FESEM), diffuse reflection spectra, photoluminescence (PL) excitation and emission spectra, quantum yield, kinetic decay, and electron paramagnetic resonance (EPR), respectively. It was found that the undoped BPO_4 showed a weak purple blue emission (409 nm, lifetime 6.4 ns) due to the carbon impurities involved in the host lattice. Doping Ba^{2+} into BPO_4 resulted in oxygen-related defects as additional emission centers which enhanced the emission intensity greatly (>10×) and shifted the emission to a longer-wavelength region (λ_{max} = 434 nm; chromaticity coordinates: $x = 0.174$, $y = 0.187$) with a bluish-white color. The highest emission intensity was obtained when doping 6 mol % Ba^{2+} in BPO_4, which has a quantum yield as high as 31%. The luminescent mechanisms of BPO_4 and Ba^{2+}-doped BPO_4 were discussed in detail according to the existing models for silica-based materials.

I. Introduction

Luminescent materials have been playing an important role in modern society for information displays and lighting.[1,2] Most of the commercially available lamp phosphors require excitation by short ultraviolet (UV) light for operation, a requirement resulting in the extensive use of a mercury vapor plasma in fluorescent lighting products.[3] In addition, the activators used in fluorescent lamp or cathodoluminescent display phosphors are often expensive or environmentally toxic metals such as silver, cadmium, and rare earth elements.[1−3] So now, much effort has been devoted to exploring novel luminescent materials that do not contain expensive or toxic elements[4−9] or do not need mercury vapor plasma as the excitation source.[2,10]

In this paper, we present a new kind of stable, efficient, and environmentally friendly luminescent material, BPO_4 doped with Ba^{2+} (instead of lanthanide or other toxic transition metal ions) prepared by the sol−gel process. This material shows an intense bluish-white emission (λ_{max} = 416−451 nm, centered at 434 nm) under a wide range of UV-light excitation (250−400 nm). The polycrystalline powder of BPO_4 is well-known as a catalyst for a range of organic chemical reactions,[11,12] and Li-doped BPO_4 has found applications as a ceramic electrolyte for Li-ion rechargeable batteries.[13] Additionally, the single crystal of BPO_4 has been investigated as a potential nonlinear optical material.[14] The crystal structure of BPO_4 is built by sharing the corner of BO_4 and PO_4 tetrahedra leading to a continuous, three-

* To whom all correspondence should be addressed. E-mail: jlin@ns.ciac.jl.cn (Prof. Jun Lin).
[†] Key Laboratory of Rare Earth Chemistry and Physics.
[‡] State Key Laboratory of Polymer Physics and Chemistry.
[§] University of New Orleans.

(1) Blasse, G.; Grabmaier, B. C. *Luminescent Materials*; Springer-Verlag: Berlin 1994.
(2) Feldmann, C.; Jüstel, T.; Ronda, C. R.; Schmidt, P. J. *Adv. Funct. Mater.* **2003**, *13*, 511.
(3) Ropp, R. C. *Luminescence and the Solid State*; Elsevier: Amsterdam, Netherlands, 1991; Vol. 12, pp 283−352.
(4) Green, W. H.; Le, K. P.; Grey, J.; Au, T. T.; Sailor, M. J. *Science* **1997**, *276*, 1826.
(5) Hayakawa, T.; Hiramitsu, A.; Nogami, M. *Appl. Phys. Lett.* **2003**, *82*, 2975.
(6) Brankova, T.; Bekiari, V.; Lianos, P. *Chem. Mater.* **2003**, *15*, 1855. Bekiari, V.; Lianos, P. *Langmuir* **1998**, *13*, 33459; Bekiari, V.; Lianos, P. *Chem. Mater.* **1998**, *10*, 3777.
(7) Yold, B. E. *J. Non-Cryst. Solids* **1992**, *147*, 614.
(8) Carlos, L. D.; Sá Ferreira, R. A.; Pereira, R. N.; Assuncão, M.; Bermudez, V. de Z. *J. Phys. Chem. B* **2004**, *108*, 14924. Carlos, L. D.; Sá Ferreira, R. A.; Bermudez, V. de Z. *Handbook of Organic−Inorganic Hybrid Materials and Nanocomposites*; Nalwa, H. S., Ed.; American Scientific Publishers: North Lewis Way, CA, 2003; Vol. 1, Chapter 9, pp 353−380. Sá Ferreira, R. A.; Carlos, L. D.; Bermudez, V. de Z. *Encyclopedia of Nanoscience and Nanotechnology*; Nalwa, H. S. Ed.; American Scientific Publishers: North Lewis Way, CA, 2004; Vol. 4, pp 719−762. Fu, L.; Sá Ferreira, R. A.; Silva, N. J. O.; Carlos, L. D.; Bermudez, V. de Z.; Rocha, J. *Chem. Mater.* **2004**, *16*, 1507. Carlos, L. D.; Bermudez, V. de Z.; Sá Ferreira, R. A.; Marques, L.; Assunção, M. *Chem. Mater.* **1999**, *11*, 581.
(9) Cordoncillo, E.; Guaita, F. J.; Escribano, P.; Philippe, C.; Viana, B.; Sanchez, C. *Opt. Mater.* **2001**, *18*, 309. Lin, J.; Baerner, K. *Mater. Lett.* **2000**, *46*, 86.
(10) Wegh, R. T.; Donker, H.; Oskam, K. D.; Meijerink, A. *Science* **1999**, *283*, 663. Toda, K. *J. Alloys Compd.* **2005**, in press.
(11) Chau, C. N.; Smith, J. A. U.S. Patent No. 5082640, 1992.
(12) Sato, S.; Hasegawa, M.; Sodesawa, T.; Nazaki, F. *Bull. Chem. Soc. Jpn.* **1991**, *64*, 516.
(13) Kelder, E. M.; Jak, M. J. G.; Lang, F.; Schoonman, J. *Solid State Ionics* **1996**, *85*, 285.
(14) Li, Z.; Lin, Z.; Wu, Y.; Fu, P.; Wang, Z.; Chen, C. *Chem. Mater.* **2004**, *16*, 2906.

10.1021/cm052109h CCC: $33.50
Published on Web 12/14/2005

dimensional framework, analogous to the appreciate SiO_2 polymorph.[11−14] However, so far no attention has been paid to the luminescence properties of BPO_4-based materials. Herein, we found that sol−gel-derived BPO_4 polycrystalline powder showed a weak purple blue luminescence (409 nm). Doping a small amount (6 mol %) of Ba^{2+} into BPO_4 resulted in a great enhancement (>10×) of the emission intensity and a red shift of the emission band (λ_{max} = 416−451 nm). Possible mechanisms have been proposed to explain the observed luminescent phenomena according to the existing models for silica-based materials.

II. Experimental Section

Preparation. Pure BPO_4 and $B_{1-x}PO_4/xBa^{2+}$ (x = 2, 4, 6, 8, 15 mol %) powder samples were prepared by a sol−gel method. Stoichiometric weights of $(NH_4)_2HPO_4$ (analytical reagent, A. R.) and $Ba(CH_3COO)_2$ (A. R.) were dissolved in a 0.01 mol/L HNO_3 (A. R.) aqueous solution under vigorous stirring. H_3BO_3 (50 mol % excess to compensate the evaporation of B at high temperature, A. R.), glycerol (A. R.), and poly(ethylene glycol) (PEG, molecular weight = 20 000, A. R.) with a molar ratio of 8:16:1 were added to 50 mL of a water/ethanol (v/v = 1:4) solution. Transparent sol was obtained after mixing the above two solutions and stirring for 3 h. The sol was dried at 100 °C to form gel powder. The obtained gel was preheated at 450 °C for 2 h, fully ground, and sintered at 1000 °C for 4 h to produce the final samples.

Characterization. The X-ray diffraction (XRD) of powder samples was examined on a Rigaku-Dmax 2500 diffractometer using Cu Kα radiation (λ = 0.15405 nm). Fourier transform infrared (FT-IR) spectra were measured with a Perkin-Elmer 580B infrared spectrophotometer with the KBr pellet technique. The morphology and composition of the samples were inspected using a field emission scanning electron microscope (FESEM, XL30, Philips) equipped with an energy-dispersive X-ray spectrum (EDS, JEOL JXA-840). Diffuse reflectance spectra were taken on a Hitachi F-4100 spectrophotometer from 200 to 800 nm. The photoluminescence (PL) excitation and emission spectra were taken on an F-4500 spectrophotometer equipped with a 150 W xenon lamp as the excitation source. Luminescence lifetimes were measured with a Lecroy Wave Runner 6100 digital oscilloscope (1 GHz) using 307 and 311 nm lasers (pulse width = 4 ns) as the excitation source (Continuum Sunlite OPO). The PL quantum yields were measured by an integrating sphere (Power Technology, Inc.) using a 325 nm HeCd laser (Kimmom, Japan) as the excitation source. Electron paramagnetic resonance (EPR) spectra were taken on the JES-FE3AX electronic spin resonance spectrophotometer. The crystal parameters and bond lengths of BPO_4 and BPO_4/Ba^{2+} were calculated using CASTEP code. [15] All the measurements were performed at room temperature.

III. Results and Discussion

XRD. Figure 1 shows the XRD patterns for the synthesized BPO_4/xBa^{2+} (x = 0, 2, 4, 6, 8, 15 mol %) as well as the standard data for BPO_4 (JCPDS No. 34-0132). As seen clearly in Figure 1, the diffraction peaks of the sol−gel-derived BPO_4 and Ba^{2+}-doped BPO_4 samples agree well with those of the standard data of BPO_4 (JCPDS No. 34-0132) and can be indexed accordingly. No other phase can be detected, indicating that the Ba^{2+} ions have been successfully dissolved in the BPO_4 host. However, with the increase of doping concentration (x) of Ba^{2+} in BPO_4, the XRD peak intensity becomes weaker. Pure BPO_4 crystallizes in tetragonal lattice, with space group $I\bar{4}$ (No. 82).[16] The crystal structure of BPO_4 is built by sharing the corner of BO_4 and PO_4 tetrahedra, leading to a continuous, three-dimensional framework, analogous to the appreciate SiO_2 polymorph (Supporting Information Figure S1).[17] A decrease in XRD peak intensity with increasing Ba^{2+}-doping level indicates removal of B and/or P from lattice sites.[18]

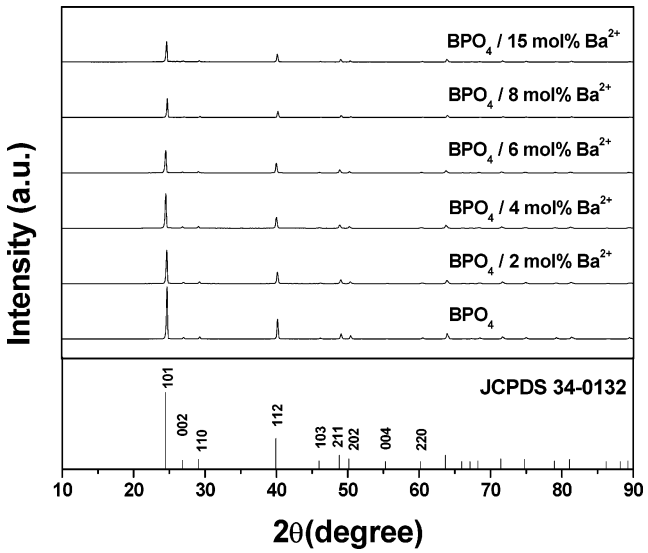

Figure 1. The XRD patterns for sol−gel-derived BPO_4/xBa^{2+} (x = 0, 2, 4, 6, 8, 15 mol %) samples and the standard data for BPO_4 (JCPDF Card No. 34-0132).

Table 1. Cell Constants and Bonding Lengths of BPO_4/xBa^{2+} (x = 0, 2, 4, 6, 8, 15 mol %) Calculated Using CASTEP Code

x (mol %)	0	2	4	6	8	15
a (Å)	4.326	4.329	4.336	4.337	4.325	4.329
c (Å)	6.627	6.627	6.635	6.640	6.624	6.630
B−O (Å)	1.459	1.460	1.462	1.463	1.459	1.460
P−O (Å)	1.524	1.525	1.527	1.528	1.524	1.525
B−P (Å)	2.725	2.726	2.730	2.731	2.724	2.726

The calculated lattice constants and bonding lengths for BPO_4/xBa^{2+} (x = 0, 2, 4, 6, 8, 15 mol %) are collected in Table 1. Basically, from Table 1, we can see that the introduction of Ba^{2+} (which is much bigger than the B^{3+}) results in the slight increase of the lattice constants and bonding lengths for BPO_4, but not very regularly. In view of the large differences of ionic radii and valence state between B^{3+} (r = 0.011 nm for 4-coordination, +3) and Ba^{2+} (r = 0.135 nm for 6-coordination, +2), it is assumed that only a very limited amount of the doped Ba^{2+} will replace the B^{3+} ions and occupy the B^{3+} sites in the host lattice.

(15) Segall, M. D.; Lindan, P. L. D.; Probert, M. J.; Pickard, C. J.; Hasnip, P. J.; Clark, S. J.; Payne, M. C. *J. Phys.: Condens. Matter.* **2002**, *14*, 2717.
(16) Achary, S. N.; Tyagi, A. K. *J. Solid State Chem.* **2004**, *177*, 3918.
(17) Adamczyk, A.; Handke, M. *J. Mol. Struct.* **2000**, *555*, 159.
(18) Jak, M. J. G.; Kelder, E. M. Schoonman, J. *J. Solid State Chem.* **1999**, *142*, 74.

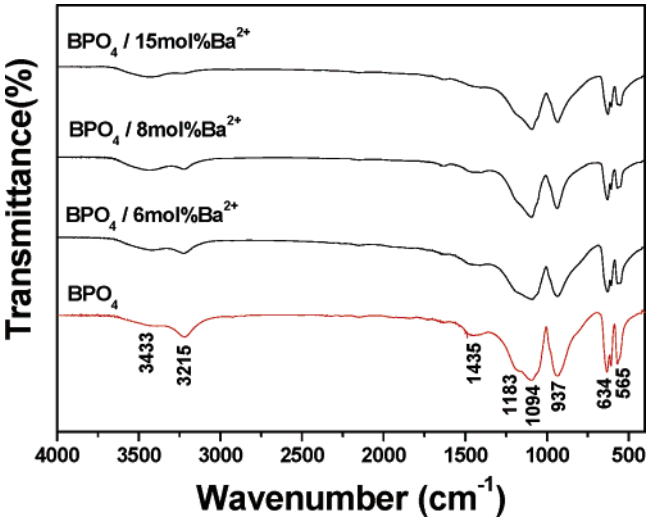

Figure 2. The FT-IR spectra for sol−gel-derived BPO_4/xBa^{2+} (x =0, 6, 8, 15 mol %)

Most of the Ba^{2+} ions will occupy the interstitial sites of the BPO_4 lattice. This is the reason the introduction of Ba^{2+} induces the slight increase of the lattice constants and bonding lengths for BPO_4 irregularly (with the increase of Ba^{2+} concentration).

FT-IR. The FT-IR spectra of BPO_4/xBa^{2+} (x = 0, 6, 8, 15 mol %) samples are shown in Figure 2. There are two different chemical bonds present in the structure of BPO_4: stronger P−O and some weaker B−O. Two groups of bands in the range of 564−633 cm^{-1} (568, 632 cm^{-1}) are due to the bending vibrations of PO_4 groups. The bands at 1094 and 1183 cm^{-1} are ascribed to the asymmetric stretching vibrations in PO_4 groups.[17] The band with a maximum at 935 cm^{-1} corresponds to the asymmetric stretching vibration of the BO_4 tetrahedron.[17] The bands at 3433 and 3215 are ascribed to the O−H vibrations of H_2O absorbed in the samples. The weak band with a maximum at 1435 cm^{-1} is due to the C−O vibration,[19] indicating that the carbon impurity has not been removed completely in the sol−gel-derived samples despite the fact that they have been annealed at high temperature (1000 °C). The carbon impurity can also be detected by energy-dispersive X-ray spectrum (EDS, see next section). From Figure 2, it can be seen clearly that the introduction of Ba^{2+} in BPO_4 resulted in the decrease of the absorption intensity of PO_4 and BO_4 groups, indicating a little amount of PO_4 and BO_4 groups in BPO_4 have been destroyed by the doped Ba^{2+}.[18] This agrees well with the results of XRD.

FESEM and EDS. Figure 3 shows the FESEM image (a) and the energy-dispersive X-ray spectrum (EDS) (b) of the BPO_4/(6 mol % Ba^{2+}) sample. From Figure 3a, we can see that the BPO_4/(6 mol % Ba^{2+}) sample is composed of aggregated particles ranging from 100 to 150 nm in size. EDS examination confirms the presence of P, O, B, and Ba from the sample and others (Si, Al, and K from the mica substrate and Au from the coating for SEM measurement). The detected carbon impurity (C, also observed in the IR spectra) is from the sample prepared by the sol−gel process

(19) Dean, J. A. *Lange*'s *Handbook of Chemistry* (Chinese version); Scientific Publisher of China: Beijing, 2003.

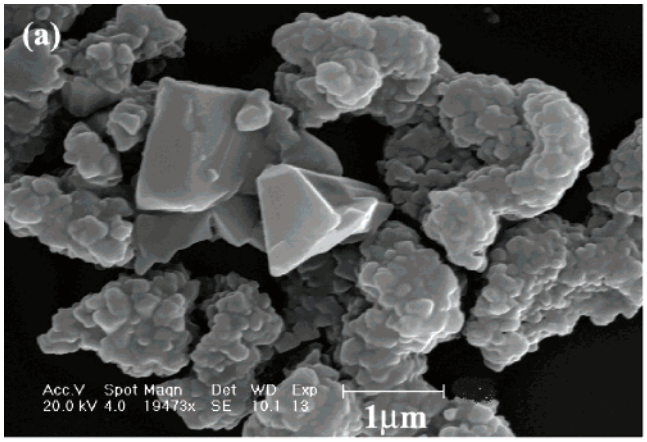

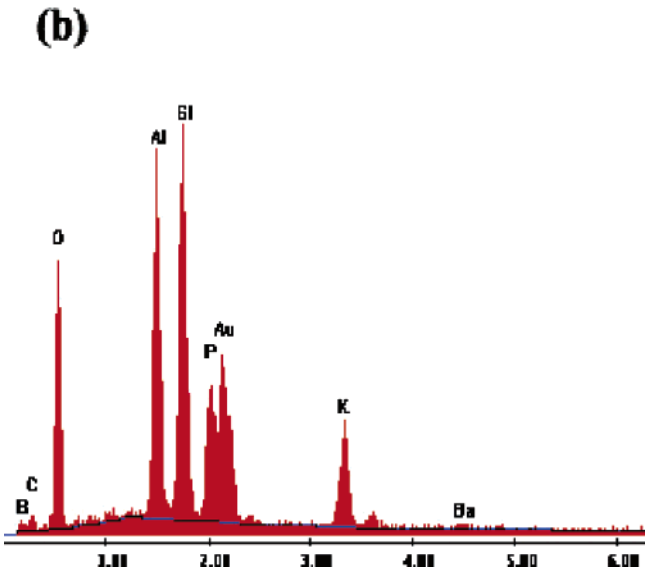

Figure 3. (a) FESEM micrograph and (b) EDS of sol−gel-derived BPO_4/(6 mol % Ba^{2+}).

in which some organic solvents and additives (glycerol and poly(ethylene glycol)) were employed.

Photoluminescence Properties. Both pure BPO_4 and BPO_4/(6 mol % Ba^{2+}) exhibit near-white color under sunlight or daylight lamp. Under UV-light irradiation, BPO_4 shows a very weak luminescence with dark purple color and BPO_4/(6 mol % Ba^{2+}) exhibits a bright bluish-white luminescence (Supporting Information Figure S2). Diffuse refection spectra (Figure 4) show that pure BPO_4 has a weak absorption band from 260 to 350 nm with a maximum at 290 nm and BPO_4/(6 mol % Ba^{2+}) has strong absorption from 230 to 600 nm with two maxima at 316 and 378 nm.

Parts a and b of Figure 5 show the excitation and emission spectra of sol−gel-derived BPO_4 and BPO_4/(6 mol % Ba^{2+}), respectively. For BPO_4, the emission spectrum consists of a weak broad band ranging from 350 to 600 nm with a maximum at 409 nm (Figure 5b, green line), and the corresponding excitation spectrum includes a broad band from 280 to 325 nm with a maximum at 307 nm (Figure 5a, green line), which basically agrees with the diffuse reflection spectrum (Figure 4, dashed line). The Stokes shift for the luminescence of BPO_4 is around 8000 cm^{-1}. Great changes were observed for luminescence properties when Ba^{2+} was

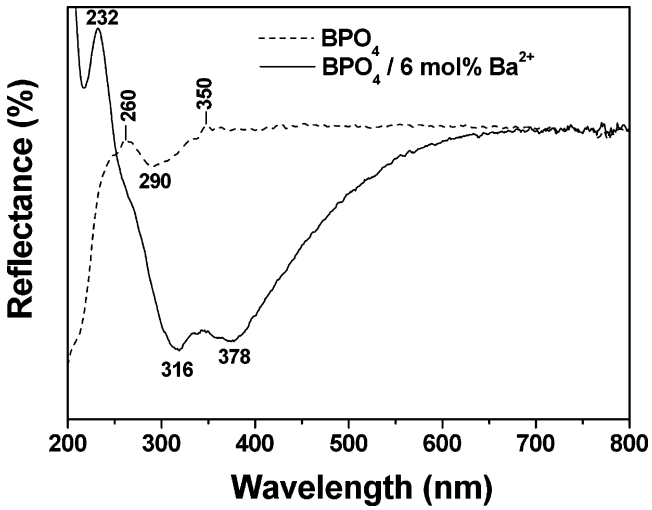

Figure 4. Diffuse reflection spectra of sol−gel-derived BPO_4 and BPO_4/6 mol %Ba^{2+}.

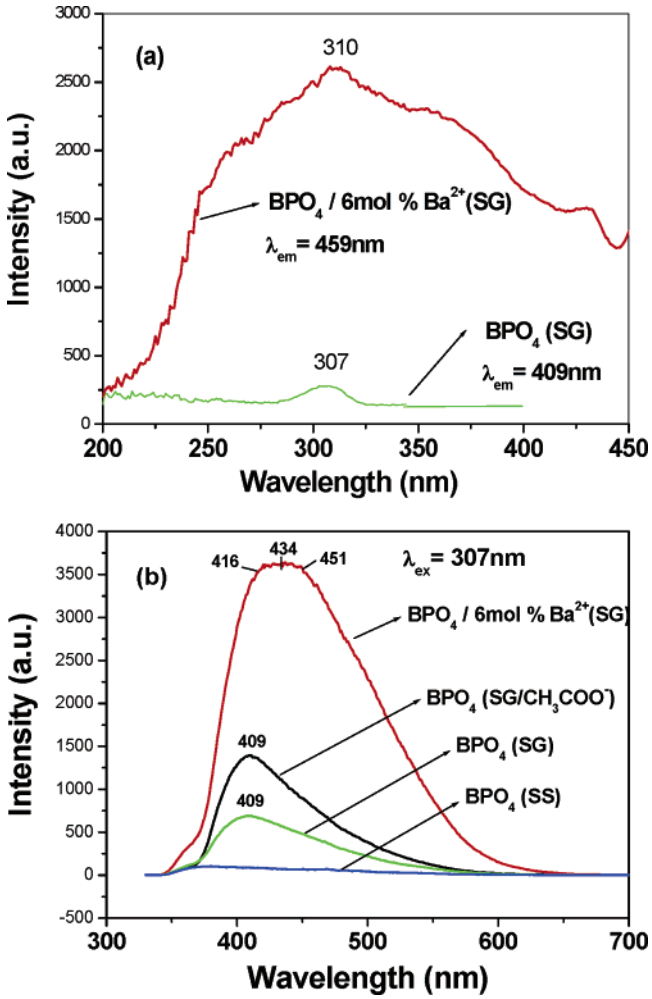

Figure 5. (a) Excitation and (b) emission spectra for BPO_4 and BPO_4/6 mol %Ba^{2+}. [SG = sol−gel; SG/CH_3COO^- = sol−gel with CH_3COONH_4 instead of $Ba(CH_3COO)_2$ as dopant; SS = solid-state reaction using H_3BO_3 and $(NH_4)_2HPO_4$]. All spectra were measured under the same instrumental conditions, so they are comparable.

doped into BPO_4. As a representative instance, the BPO_4/(6 mol % Ba^{2+}) sample shows a very strong emission band peaking from 416 to 451 nm (centered at 434 nm) (Figure 5b, red line), whose integrated intensity is enhanced >10× with respect to that of pure BPO_4. The shoulder at 416 nm

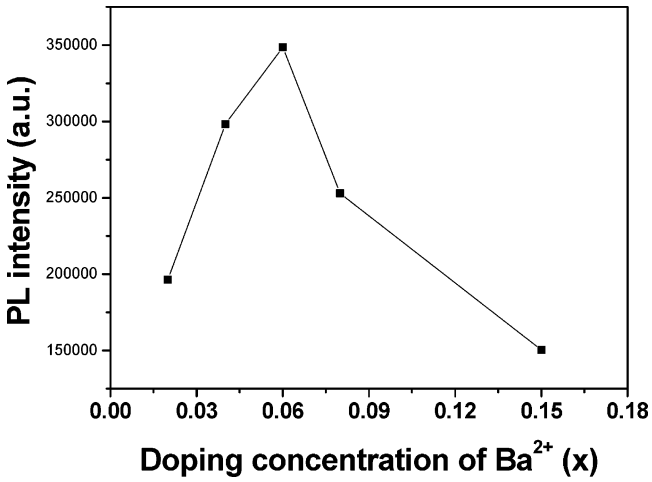

Figure 6. The emission intensity of sol−gel-derived BPO_4/xBa^{2+} as a function of Ba^{2+} concentration (x, in mol).

is probably from the same emission centers as those in the undoped BPO_4, and the main peak at 434 nm is from new emission centers created by the Ba^{2+} doping. Basically in agreement with the diffuse reflection spectrum in Figure 4 (solid line), the excitation spectrum of BPO_4/(6 mol % Ba^{2+}) contains a very strong and broad band ranging from 220 to 450 nm with a maximum at 310 (Figure 5a, red line). The excitation for BPO_4/(6 mol % Ba^{2+}) is greatly broadened and intensified in comparison with that for pure BPO_4, i.e., the BPO_4/(6 mol % Ba^{2+}) sample can be easily excited by the light from 250 to 450 nm, leading to the strong bluish-white emission. The Stokes shift for the luminescence of BPO_4/(6 mol % Ba^{2+}) amounts to 10 000 cm^{-1}, a value a little larger than that (8 000 cm^{-1}) for BPO_4. The chromaticity coordinates (CIE) of BPO_4/(6 mol % Ba^{2+}) are $x = 0.174$, $y = 0.187$.

To understand and optimize the luminescent properties of Ba^{2+}-doped BPO_4, experiments to determine the effects of the doping concentration of Ba^{2+} were performed. It is found that the shape and profile for the emission and excitation spectra do not vary with the change of the Ba^{2+}-doping concentration, but the integrated PL intensity changes greatly, as shown in Figure 6. The PL intensity first increases with increasing Ba^{2+} concentration (x), reaching a maximum at x = 6 mol %, then decreases quickly with further increasing Ba^{2+} concentration. Thus, the optimum doping concentration of Ba^{2+} was determined to be 6 mol % for obtaining the strongest PL emission intensity. The excitation and emission spectra of Ba^{2+}-doped BPO_4 have much overlap (parts a and b of Figure 5), so there should be a great probability of energy transfer among the emission centers. This energy transfer will result in luminescence quenching when the concentration of the emission center is high enough. [1] Thus, it is understandable that there is an optimum concentration of Ba^{2+} (which brings about the emission centers) for obtaining the strongest PL emission intensity.

The PL quantum yield and kinetic properties were further studied for BPO_4/(6 mol % Ba^{2+}) with respect to the undoped BPO_4 sample. It is found that the PL quantum yield for undoped BPO_4 is ~17%, while that of BPO_4/(6 mol % Ba^{2+}) is as high as 31% under the excitation of 325 nm HeCd laser. The PL quantum yield of BPO_4/(6 mol % Ba^{2+}) is a pretty

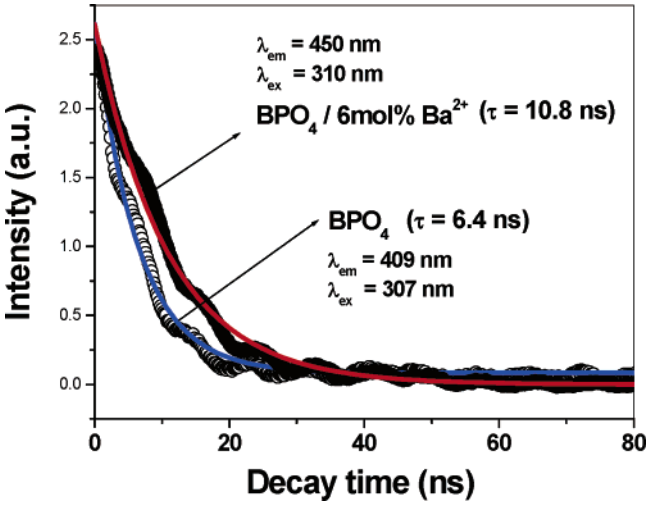

Figure 7. The decay curves for the luminescence of sol−gel-derived BPO_4 and BPO_4/6 mol %Ba^{2+} samples.

high value among the phosphor family without metal activators.[8] For example, the APTES (3-aminopropyl)-triethoxysilane) hybrid with formic acid is one of the most efficient phosphors known among those not containing activator metal ions, with a PL quantum yield ∼35%.[4]

The luminescence decay curves for BPO_4 and BPO_4/(6 mol % Ba^{2+}) are shown in Figure 7. Both of them can be fitted to a single-exponential function as $I = I_0 \exp(-t/\tau)$ (τ is lifetime), from which the lifetimes are determined to be 6.4 ns for BPO_4 and 10.8 ns for BPO_4/(6 mol % Ba^{2+}), respectively. Note that the lifetime of BPO_4/(6 mol % Ba^{2+}) becomes longer than that of BPO_4, indicative of different emission centers existing in these two kinds of samples.

Possible Luminescence Mechanisms. Since no literature concerning the luminescence of BPO_4-based materials can be found, the luminescent mechanisms for the sol−gel-derived BPO_4 and Ba^{2+}-doped BPO_4 are not very clear at this stage. Herein, we can only explain the above luminescent phenomena according to the existing models. Because Ba^{2+} ([Kr] $4d^{10}5s^25p^6$ electronic configuration, no single electron) itself is not able to show luminescence, the observed luminescence from BPO_4 and Ba^{2+}-doped BPO_4 must be related to some impurities and/or defects in the host lattice, which can be confirmed by the short lifetimes: 6.4 ns for pure BPO_4 and 10.8 ns for BPO_4/(6 mol % Ba^{2+}), typical values for the luminescence caused by defects.[20,21]

As stated previously, the crystal structure of BPO_4 consists of BO_4 and PO_4 tetrahedra like the SiO_4 tetrahedral framework in crystalline or amorphous SiO_2 (including SiO_2 glass,[4,5,7] SiO_2 gels,[4,9] organic/inorganic hybrid silicones,[6,8] silica nanotubes,[22] etc.), which are well-known to show luminescence generally from the blue to red spectral region. Moreover, molecular sieves such as MCM-41[23] and MCM-48,[24] open-framework phosphates and germinates, [25] as well as porous zinc gallophosphates [26] show excellent and tunable luminescence properties in the visible region. In all of the above materials, the origins of the luminescence have been ascribed to defects and/or impurities in the hosts without clear and exact identification of emission centers.

Before elucidating the possible luminescent mechanisms for the sol−gel-derived BPO_4 and Ba^{2+}-doped BPO_4, let us review those of SiO_2-based materials briefly. For room-temperature-obtained organic/inorganic hybrid silicones containing $-NH_2$ (or $-NH$) groups, Carlos et al. proposed a mechanism based on NH_3^+/NH^- (or NH_2^+/N^-) donor−acceptor pairs to explain the blue emission from these materials.[8] Another defect type associated with carbon impurities was proposed as being the origin of the luminescence of sol−gel-derived silica gels based on tetraethyl orthosilicate (TEOS) and tetramethoxysilane (TMOS) incorporating a variety of carboxylic acids.[4] Under adequate heat treatments (at least above 520 K), a carbon impurity is created in the $-O-Si-O-$ network forming $-O-C-O-$ and/or $-Si-C-$ bonds. The carbon-related defects are only luminescent active after a heat treatment, because these xerogels are not luminescent prior to this procedure.[8] Other intrinsic defect sites that are known to bring about the luminescence of SiO_2 (glasses, gels, hybrid silicones, or nanotubes, as well as MCM molecular sieves) include E′-type luminescent centers ($^{\bullet}Si\equiv$, an unpaired electron on a silicon-dangling bond, where the spin is highly localized in the silicon atom), nonbridging oxygen hole center (NBOHC, usually denoted by $^{\bullet}O-Si\equiv O3$), and the peroxy-radical hole trap (PRHT, $^{\bullet}O-O-Si\equiv O3$).[7−9,23,24] Each of the defect sites has a characteristic photoluminescence when excited with high-energy photons ($h\nu > 3.5$ eV or $\lambda < 357$ nm): 459 nm for PRHT,[27] 288 nm for E′-type centers, [28] and 652−670 nm for NBOHC. [29]

Now we try to clarify the possible luminescent mechanisms in our sol−gel-derived BPO_4 and Ba^{2+}-doped BPO_4 samples. For the sol−gel-derived undoped BPO_4, we assume the weak, purple blue luminescence is mainly from the carbon impurities as those of sol−gel-derived silica gels based on TEOS and TMOS incorporating a variety of carboxylic acids (denoted as "C−SiO_2 gels" later).[4] We have the following evidence to support this conclusion. First, the profile of the emission spectrum (emission range = 350 to 600 nm, λ_{max} = 409 nm) and the PL lifetime (6.4 ns) of our sol−gel-derived undoped BPO_4 are similar to those of C−SiO_2 gels (emission range = 350−700 nm, λ_{max} varies between 405 and 550 nm depending on the preparation conditions; PL lifetime < 10 ns).[4] Second, carbon element has been detected by FT-IR spectra (Figure 2) and EDS in

(20) Fujimaki, M.; Ohki, Y.; Nishikawa, H. *J. Appl. Phys*. **1997**, *81*, 1042.
(21) Pifferi, A.; Taroni, P.; Torricelli, A.; Valentini, G.; Mutti, P.; Ghislotti, G.; Zanghieri, L. *Appl. Phys. Lett*. **1997**, *70*, 348.
(22) Jang, J.; Yoon, H. *Adv. Mater*. **2004**, *16*, 799.
(23) Gimon-Kinsel, M. E.; Groothuis, K.; Balkus, K. J., Jr. *Microporous Mesoporous Mater*. **1998**, *20*, 67.
(24) Lee, Y. C.; Liu, Y. L.; Shen, J.-L.; Hsu, I. J.; Cheng, P. W.; Cheng, C. F.; Ko, C.-H. *J. Non-Cryst. Solids* **2004**, *341*, 16.
(25) Feng, P. *Chem. Commun*. **2001**, 1668.
(26) Liao, Y. C.; Lin, C. H.; Wang, S. L. *J. Am. Chem. Soc*. **2005**, *127*, 9986.
(27) Guzzi, M.; Martini, M.; Pio, F.; Spinolo, G.; Vedda, A. *The Physics and Technology of amorphous SiO2*; Devine, R. A. B., Ed.; Plemum Press: New York, 1988; p 175.
(28) Imai, H.; Arai, K.; Saito, T.; Ichimura, S.; Nonaka, H.; Vigouroux, J. P.; Imagawa, H.; Hosono, H.; Abe, Y. *The Physics and Technology of amorphous SiO2*; Devine, R. A. B., Ed.; Plemum Press: New York, 1988; p 153.
(29) Munekuni, S.; Yamanaka, T.; Shimogaichi, Y.; Nagasawa, K.; Hama, Y. *J. Appl. Phys*. **1990**, *68*, 1212.

Scheme 1. Excitation and Emission Process Induced by C Impurity in BPO_4

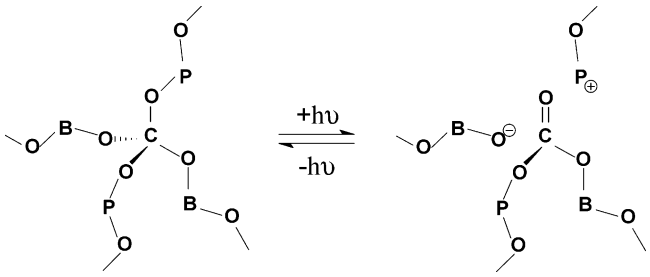

Scheme 2. Simple Process for the Production of Peroxyl Radicals in BPO_4 by Ba^{2+} Doping

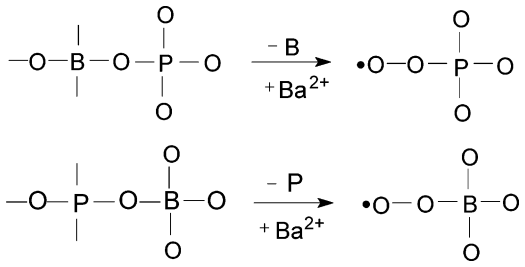

our sol−gel-derived Ba^{2+}-doped (Figure 3b) and undoped BPO_4 (not shown). To check the effects of carbon impurity, we prepared a pure BPO_4 sample by simply mixing H_3BO_3 and $(NH_4)_2HPO_4$ powders and firing them at high temperature (1000 °C), i.e., the solid-state reaction (SS) process (without using any organic solvents and additives, thus no carbon impurity involved). This SS-derived BPO_4 without carbon impurity did not show any luminescence under the same excitation condition (Figure 5b, blue line). Moreover, keeping all other conditions same, we also prepared a BPO_4 sample by the sol−gel process using CH_3COONH_4 as additive instead of $Ba(CH_3COO)_2$. It is assumed that more carbon impurities will be included in this sol−gel-derived BPO_4 sample. Indeed, this sample shows similar emission spectrum to that of sol−gel-derived BPO_4 without using CH_3COONH_4 as additive, but the former (Figure 5b, black line) has a higher emission intensity than the latter (Figure 5b, green line). From the above results, we can safely conclude that the weak, dark purple emission in sol−gel-derived BPO_4 is from the carbon impurities in the host lattice. In the preparation of BPO_4 via the sol−gel process, glycerol and PEG were employed as additives which contain large amounts of carbon. In the subsequent annealing process, most of the additives decomposed into H_2O and CO_2 and escaped from the system, but minor amounts of them may decompose to create a carbon-substitutional defect for B or P atom, which is assumed to be the luminescent species in the lattice (like −O−B−C−O−P−O−). Considering the dissociation energies for C—O (1076 kJ/mol), C═O (749 kJ/mol), B—O (806 kJ/mol), and P—O (597 kJ/mol) bonds, [19] the luminescence process can be expressed in Scheme 1.[4]

Compared with BPO_4, the excitation and emission spectra as well as the PL lifetime of Ba^{2+}-doped BPO_4 change greatly, as stated in the previous section. This indicates that additional emission centers have been created by doping Ba^{2+} into the BPO_4 host lattice. Since Ba^{2+} itself cannot luminesce, the emission center must be related to some new defects different from the carbon impurities. Note that a very similar situation was reported by Gu et al.,[30] who found that the introduction of Ce^{3+} in SnO_2 could significantly enhance the photoluminescence intensity of SnO_2, in which the luminescence is considered a result of oxygen vacancies. The role of Ce^{3+} is to increase the amount of oxygen vacancies in SnO_2 and, thus, increase the emission intensity.

Considering the similar structure between BPO_4 and SiO_2, the E′-type, NBOHC, and PRHT defect centers in SiO_2 are also possible to be created in the BPO_4 lattice by the effect of Ba^{2+} doping. On the basis of the basic emission characteristics of these defects (E′-type = 288 nm, NBOHC = 652−670 nm, and PRHT = 459 nm) and the emission spectrum of Ba^{2+}-doped BPO_4 (λ_{max} = 434−450 nm), the E′-type and NBOHC defects can be ruled out as the luminescent centers in Ba^{2+}-doped BPO_4. Furthermore, these two kinds of defects have been generally assumed as the emitting centers in the cases of organic/inorganic hybrid silicone gels. Ba^{2+}-doped BPO_4 was prepared by sintering at 1000 °C. Therefore, the E′-type and NBOHC defects are not plausible for the luminescent centers in crystalline Ba^{2+}-doped BPO_4. As a result, according to the emission properties, the most probable new luminescent center in the crystalline Ba^{2+}-doped BPO_4 is PRHT (peroxy-radical hole trap, •O−O−P≡O3 and/or •O−O−B≡O3). Because of the large difference (valence state and ionic radii) between Ba^{2+} and B^{3+} (P^{5+}), the introduction of Ba^{2+} in BPO_4 will disturb the frame structure of BO_4 and PO_4 tetrahedra to a great extent, i.e., some of the B and P atoms have been removed from the BO_4 and PO_4 tetrahedra, as evidenced by the XRD and FT-IR spectra.[18] It also can be imagined that the big "Ba^{2+}" ions will squeeze the B and/or P atoms out of their normal lattice sites in BPO_4 and destroy the BO_4 and PO_4 tetrahedra. When the B or P was removed from the lattice site, it is very possible to produce •O−O−P≡O3 or •O−O−B≡O3 defects. The process can be simply expressed as Scheme 2. To prove the proposed assumption, EPR spectra for undoped BPO_4 and BPO_4/(6 mol %Ba^{2+}) were measured. No obvious EPR signal was observed for the undoped BPO_4, while BPO_4/(6 mol % Ba^{2+}) exhibits a strong and sharp EPR band at g = 2.001 (Figure 8). This indicates that there indeed exist paramagnetic defects in BPO_4/(6 mol % Ba^{2+}). Since

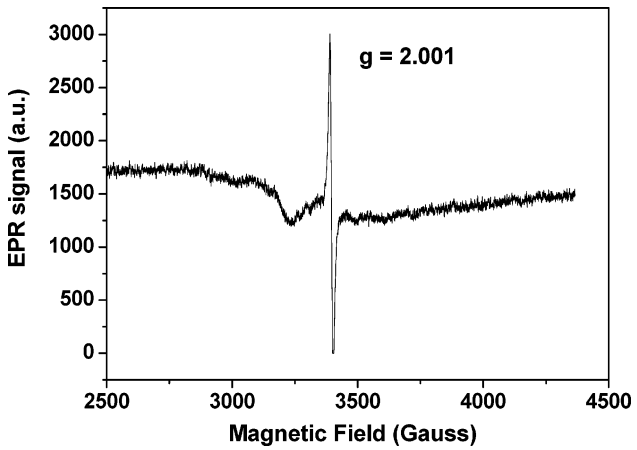

Figure 8. The EPR spectrum for sol−gel-derived BPO_4/6 mol %Ba^{2+}.

(30) Gu, F.; Wang, S.; Lü, M.; Zhou, G.; Xu, D.; Yuan, D. *J. Phys. Chem. B* **2004**, *108*, 8119.

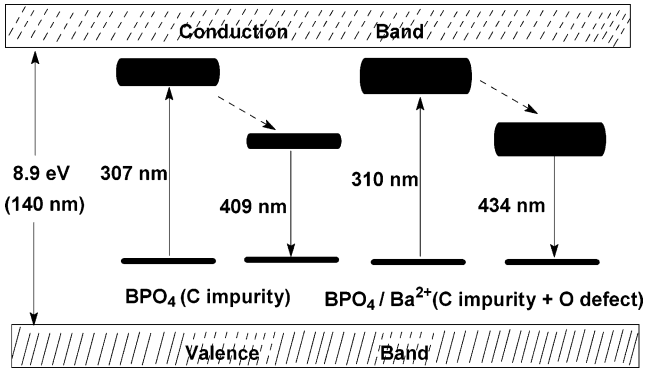

Figure 9. Energy band diagram showing the possible defects and emission process in sol−gel-derived BPO_4 and BPO_4/Ba^{2+}

the EPR signal cannot be caused by B^{3+}, P^{5+}, and Ba^{2+} (no single electron in these ions), it must arise from some oxygen-related defects, such as peroxyl radicals.[8] As the luminescent centers of the bluish-white emission in Ba^{2+}-doped BPO_4, the oxygen defects will increase with the increase of the doping content of Ba^{2+}, and the emission intensity also increases accordingly. However, at higher concentrations of Ba^{2+} (> 6 mol %), the energy transfer among the emission centers will result in quenching of the luminescence (Figure 6). Additionally, to gain further confidence about the proposed luminescent mechanism, other alkaline earth metal ions, such as Sr^{2+}, Ca^{2+}, and Mg^{2+}, were tested to be doped into a BPO_4 host in the same way as that for Ba^{2+} (similar starting materials with identical doping concentration, 6 mol %). Under UV (310 or 365 nm) excitation, all the samples display similar luminescence properties, with BPO_4/6 mol %Ba^{2+} having the highest PL intensity (Supporting Information Figure S3). Because Ba^{2+} is larger than the other alkaline earth metal ions (Sr^{2+}, Ca^{2+}, and Mg^{2+}), it is expected that structural disturbance of BPO_4 by Ba^{2+} is greater than that by other alkaline earth metal ions. Consequently, more oxygen defects such as peroxyl radicals will be created in Ba^{2+}-doped BPO_4 than in BPO_4 doped with other alkaline earth metal ions, leading BPO_4/Ba^{2+} to be the most efficient one among this family.

In an ideal BPO_4 lattice, only B−O and P−O bonds (all B and P sites being four-coordinate and all O sites being two-coordinate) are present with a band gap around 8.9 eV and will not show any luminescence.[14] The presence of structural defects will introduce electronic states into the band gap, resulting in luminescence of this material. As a summary, the whole emission process in our sol−gel-derived undoped BPO_4 and Ba^{2+}-doped BPO_4 is schematically shown in Figure 9.

IV. Conclusions

Polycrystalline BPO_4 and Ba^{2+}-doped BPO_4 powder samples have been successfully prepared by the sol−gel process using glycerol and poly(ethylene glycol) as additives followed by high temperature (1000 °C) annealing. The undoped BPO_4 shows a weak, purple blue emission (409 nm) due to the carbon impurities involved in the host lattice. Doping Ba^{2+} into BPO_4 results in oxygen-related defects (most probably peroxyl radicals) as additional emission centers which enhance the emission intensity greatly (>10×) and shift the emission to the blue region (λ_{max} = 416−451 nm, centered at 434 nm). The optimum doping concentration of Ba^{2+} is 6 mol % in BPO_4, which has a quantum yield as high as 31%. This phosphor can be potentially used as a new efficient and environmentally friendly bluish-white luminescent material.

Acknowledgment. This project is financially supported by the foundation of "Bairen Jihua"of Chinese Academy of Sciences, the MOST of China (No. 2003CB314707), the National Natural Science Foundation of China (50225205, 20431030, 50572103), and the foundation of Jilin Province for distinguished young scholars (2001). J.F. is grateful for the financial support by the foundation of a two-base program for international cooperation of NSFC (00310530) related to Project 50225205 and NSF DMR-0449580. We are grateful for Prof. Dongge Ma and Mr. Weidong Wang (Changchun Institute of Applied Chemistry) for their kind help in the measurement of quantum efficiencies. We also thank Prof. Zhijian Wu (Changchun Institute of Applied Chemistry) for his guidance in calculating the bond lengths.

Supporting Information Available: Figures S1−S3 (PDF format) are included in the Supporting Information. This material is available free of charge via the Internet at http://pubs.acs.org.

CM052109H